# A Figure of Merit in a Time-Modulated Array

Mohammad Hossein Mazaheri [ID], Mohammad Fakharzadeh [ID], *Senior Member, IEEE*,
Mahmood Akbari, and Safieddin Safavi-Naeini [ID], *Fellow, IEEE*

*Abstract*—In this letter, we use *G/T* as a figure of merit to evaluate the performance of time-modulated arrays (TMA). The noise performance of a receiver, which is periodically switched ON and OFF, is quite different from that of a conventional receiver. We analytically investigate the noise performance of a TMA. Based on this analysis, the figure of merit, $G/T$, of the TMA structure is investigated, including the details of the receiver hardware. Moreover, the $G/T$ of the TMA is compared with that of a phased array. The comparison indicates that the TMA structure provides the same or even better performance compared to a phased array system, which demonstrates the capability of TMA in providing reasonable $G/T$ as a low-cost beamforming structure.

*Index Terms*—Antenna array, beamforming, efficiency, noise figure, time-modulated array (TMA).

## I. Introduction

THE ever-increasing demand for robust, low-power, and low-cost wireless transceivers requires development of new system architectures as well as precise analysis of the existing solutions. Particularly, wireless receivers must be capable of handling weak signals in the presence of noise and interference. Accordingly, the receiver noise performance is an important parameter of the wireless link design. An effective technique to reduce the external noise and interference is to steer the beam toward the transmitter and suppress the interference. Recently, low-cost and low-power architectures are introduced to implement the beam steering, suitable for consumer electronics.

Time-modulated array (TMA) has been known as a low-cost beamforming structure, which is promising for future wireless communication systems. Generally, high-speed RF switches are used instead of costly phase shifters to electronically steer and shape the radiation pattern [1]. The RF switches are periodically turned ON and OFF, creating sidebands in addition to the fundamental frequency. Usually, beam steering is performed with sidebands by designing proper switching sequences [2], which can both steer and shape the radiation pattern of the array. If the carrier frequency (fundamental frequency) is $f_0$ and the signal bandwidth is $B$, then the switching frequency must be higher than the signal bandwidth and much lower than the carrier frequency ($B < f_p << f_0$) to avoid aliasing and modulation distortion.
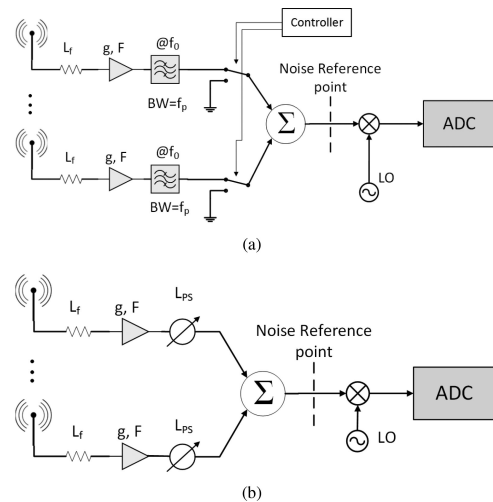
Fig. 1. Receiver architecture for (a) TMA and (b) phased array systems.

The capability of the TMA to provide simultaneous radiation patterns facilitates implementing a smart wireless communication network [3]. For a receiver, the noise performance is one of the most important parameters. Examples of the receiving array are presented in [4]–[6], where a linear array is periodically switched to estimate the direction of arrival of an unknown transmitter. Moreover, the TMA structure is used in [7] as a receiver with additional diversity to decrease the bit error rate of the receiver. The received signal-to-noise ratio (SNR) in a TMA structure is investigated in [8]. However, [8] does not consider the details of the receiver architecture and utilizes a single low noise amplifier (LNA) after the switch network, similar to [9] and [10]. Although this architecture provides low power consumption, it significantly reduces the $G/T$ in the receiver.

In this letter, we investigate the noise performance of the TMA. To reduce the noise effect in the receiver, we propose to use LNA before the switch elements. Moreover, a bandpass filter is utilized to avoid the noise folding, which usually happens in a periodically switched system. In Section II, the signal gain over equivalent noise temperature ($G/T$) of the array is calculated both at the fundamental frequency and the sidebands to characterize the performance of a TMA receiver. To bring sufficient insights, the $G/T$ of the TMA is compared with that of the phased array, considering practical hardware systems.

## II. $G/T$ Calculation for TMA

The architecture of TMA in receiving mode is shown in Fig. 1(a), where bandpass filters are used after the LNA to filter the noise spectrum and avoid the noise folding effect. According to Fig. 1(a), each single-pole double-throw (SPDT) switch is

independently controlled by a central digital processor to achieve the desired radiation pattern.

The array factor of an $N$ element TMA is [3]

$$AF_s(\theta, t) = \sum_{n=0}^{N-1} h_n(t)e^{jk_0 nd \sin \theta} \tag{1}$$

where $k_0$ is the wavenumber in free space, $d$ is the interelement spacing in the array, and $h_n(t)$ is the switching sequence of the $n$th element. Accordingly, $h_n(t)$ is a periodic train of rectangular pulses in time domain, which can be explained by Fourier coefficients $(a_{mn})$ as follows:

$$h_n(t) = \sum_{m=-\infty}^{\infty} a_{nm}e^{jm\omega_p t} \tag{2}$$

where $\omega_p$ is the frequency of the switching sequence, so

$$a_{nm} = \frac{1}{T_p} \int_0^{T_p} h_n(t)e^{-jm\omega_p t}dt. \tag{3}$$

Thus, the array factor of the TMA at the $m$th sideband is

$$AF_s(\theta, t)\Big|_m = \sum_{m=-\infty}^{\infty} e^{j(\omega_0 + m\omega_p)t} \sum_{n=0}^{N-1} a_{nm}e^{jk_0 nd \sin \theta}. \tag{4}$$

In [11] and [12], it is shown that the signal from the sidelobe directions gets distorted. Here, we assume that the communication is established through the main beam, so no distortion happens to the signal.

The efficiency of the TMA is lower than a conventional array since the antenna elements are periodically turned OFF. This issue was addressed in [3], where an efficient switching technique was proposed for a multiuser wireless link. In the receiver side, the efficiency translates into SNR, or equivalently the $G/T$. To explore the $G/T$ of the system, the system noise temperature should be investigated.

*A. Noise in Switched Network*

According to Fig. 1(a), the SPDT is connected to the ground when the antenna turns OFF. The noise generated by the ground is comparably lower than the noise of the receiver chain. Therefore, the noise of the chain experiences the same transfer function, and it is also modulated by the SPDT switching sequence

$$\mathbb{R}_{nn}(t, t+\tau) = \mathbb{E}\left\{ \left[ n_f(t) * h(t) \right] \left[ n_f(t+\tau) * h(t+\tau) \right] \right\} \tag{5}$$

where $n_f(t)$ is the noise of the chain, filtered by the bandpass filter. The bandwidth of the filter is equal or lower than $f_p$ to avoid noise folding in the receiver [13]. Accordingly, the output noise spectrum is

$$N_{br}^{(n)}(f) = \int_{-\infty}^{\infty} \mathbb{R}_{nn}(\tau)e^{-j2\pi f\tau}d\tau$$

$$= \sum_{m=-\infty}^{\infty} N_f(f + mf_p)|a_{mn}|^2 \tag{6}$$

where $N_f(f)$ is the power spectrum of the filtered noise and $a_{mn}$ is the Fourier coefficient, described in (3).

Similar to [14], we assume uncorrelated noise in each branch, so the output noise spectral density at the summation point (reference point) is

$$N_{\text{out}}(f + mf_p) = \sum_{n=0}^{N-1} N_{br}^{(n)}(f + mf_p)$$

$$= \sum_{n=0}^{N-1} N_f(f + mf_p).|a_{mn}|^2$$

$$= N_f(f + mf_p) \sum_{n=0}^{N-1} |a_{mn}|^2. \tag{7}$$

The result in (7) states that the noise signal is modulated with the corresponding switching sequence. Therefore, the equivalent noise temperature of the TMA becomes

$$T_{\text{out}}(m) = T_{\text{on}}^e \sum_{n=0}^{N-1} |a_{mn}|^2 \tag{8}$$

where $T_{\text{on}}^e$ is the equivalent noise temperature of the chain when the SPDT is ON

$$T_{\text{on}}^e = \frac{g}{L_f L_{bp} L_{sw}}T_i + \frac{g(L_f - 1)}{L_f L_{bp} L_{sw}}T_0 + \frac{g(F - 1)}{L_{bp} L_{sw}}T_0$$

$$+ \frac{L_{bp} - 1}{L_{bp} L_{sw}}T_0 + \frac{(L_{sw} - 1)}{L_{sw}}T_0 \tag{9}$$

where $L_f$, $L_{bp}$, and $L_{sw}$ are the feed loss, insertion loss of the bandpass filter, and insertion loss of the SPDT, respectively. Moreover, $g$ and $F$ represent the gain and the noise figure of the LNA. The sky noise temperature is shown by $T_i$, and $T_0$ indicates the room temperature.

The gain of the TMA, including the array factor and the gain of the chain, is

$$G = \frac{g}{L_f L_{bp} L_{sw}}|AF_s(\theta, t)|^2 = G_{br}|AF_s(\theta, t)|^2. \tag{10}$$

As a result, the $G/T$ of the TMA is

$$\frac{G}{T}\Big|_m = \frac{G_{br}|AF_s(\theta, t)|^2}{T_{\text{on}}^e \sum_{n=0}^{N-1} |a_{mn}|^2} = \eta \frac{G_{br}}{T_{\text{on}}^e} \tag{11a}$$

$$\eta = \frac{\sum_{p=0}^{N-1} \sum_{q=0}^{N-1} a_{mp}.a_{mq}^* e^{jk_0 pd \sin \theta} e^{-jk_0 qd \sin \theta}}{\sum_{n=0}^{N-1} |a_{mn}|^2} \tag{11b}$$

where $\eta$ is the switching efficiency of the TMA in its receive mode. This efficiency is a measure of the $G/T$ performance in a receiver as compared to its maximum value. To provide an insight on the noise of the TMA, a switched array with practical components is considered in the following.

*B. Numerical Study*

Assume a linear array with 16 elements having half-wavelength spacing between the elements. To compare the performance of the TMA with a conventional beamforming architecture, a radiation pattern with $-30$ dB sidelobe level (SLL) is designed through Taylor pattern tapering. Moreover, the main beam is steered toward $30°$ from the broadside. The procedure of translating the array weights (Taylor tapering) into the switching
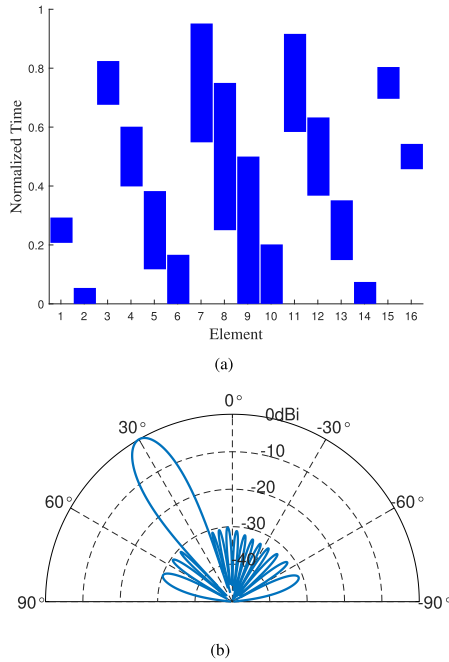
(a)



(b)

Fig. 2.   (a) Synthesized switching sequence for the desired Taylor tapering and beam steering at the first sideband. (b) Radiation pattern of the TMA at the first sideband, pointing to $30°$ with $-30$ dB SLL.

TABLE I
CHARACTERISTICS OF THE TMA COMPONENTS

| Component | Insertion loss/ Gain (dB) | Noise Figure (dB) |
|---|---|---|
| Antenna Feed | 0.5 | 0.5 |
| LNA [16] | 10 | 3 |
| Bandpass Filter | 3 | 3 |
| SPDT [17] | 0.7 | 0.7 |

sequence is explained in [15]. The switching sequence and the corresponding radiation pattern at the first sideband are shown in Fig. 2(a) and (b), respectively. Note that to achieve that SLL, the array turns OFF for a specific duration, thus the array gain reduces. This is similar to the amplitude tapering in a phased array.

Consider a TMA receiver at the S-band, including LNA, bandpass filter, and SPDT switch, similar to Fig. 1(a). The noise characteristics of these components are summarized in Table I. In addition, we assume that the input noise temperature is equal to the room temperature ($T_i = T_0$). The $G/T$ of a TMA system is calculated using (11) for different LNA gains. In addition to the TMA, the normalized $G/T$ of the phased array is shown in Fig. 3 for three different values of phase shifter insertion loss. The maximum $G/T$ of the TMA is chosen as the reference to normalize the $G/T$ of the phased array. The TMA provides slightly better $G/T$ compared to that of the phased array with 6 dB insertion loss in the phase shifter. Increasing the gain of the LNA reduces this difference, where at 25 dB gain, all of the systems provide almost the same $G/T$. Accordingly, the TMA provides an acceptable $G/T$ to be used as a receiver in a wireless communication system. To compare the $G/T$ of the phased array and lossy TMA in details, we define $\Delta G/T$ as

$$\Delta \frac{G}{T} = \frac{G}{T}\bigg|_{\text{TMA}} - \frac{G}{T}\bigg|_{\text{phasedarray}}. \qquad (12)$$

This parameter, which is shown in Fig. 4, investigates the $G/T$ variation across the insertion loss of both the SPDT and
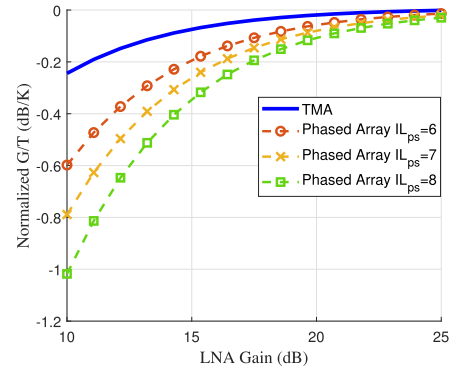


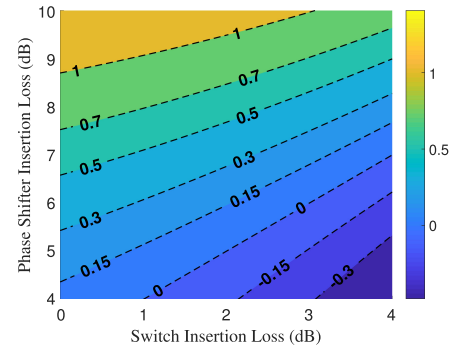Fig. 3.   $G/T$ of the switched array and the equivalent phased array versus LNA gain.



Fig. 4.   Difference between $G/T$ of the TMA and phased array versus phase shifter and SPDT loss.

TABLE II
$G/T$ VARIATION OVER SIDEBANDS AND SLLs

|  | SLL= -15 | SLL= -20 | SLL= -30 | SLL= -40 |
|---|---|---|---|---|
| m=1 | 0 | -0.177 | -0.638 | -0.974 |
| m=2 | 0 | -0.177 | -0.638 | -0.974 |
| m=3 | 0 | -0.177 | -0.638 | -0.974 |

the phase shifter. The zero contour shows where the TMA and phased array systems provide the same $G/T$. For example, a TMA with a SPDT having 0.5 dB insertion loss provides better $G/T$ than a phased array with 4 dB insertion loss of phase shifter, when the gain of the LNA is 10 dB in both systems. In other words, the internal noise, produced by RF components in TMA, is lower than that of the phased array, if the total insertion loss of a SPDT and filter is lower than the insertion loss of a phase shifter. Generally, this condition usually is met, and as a result, the TMA produces less noise than a phased array system and provides higher G/T.

To investigate the dependence of $G/T$ on design parameters, in Table II, we calculated the $G/T$ for different SLLs and at different sidebands. Here, we have normalized all values to the maximum, which corresponds to SLL equal to $-15$ dB. As presented, the $G/T$ varies with SLL since the aperture efficiency varies as well. However, according to (11b), the array efficiency does not change with sideband number, so the $G/T$ is the same for all sidebands.

## III. CONCLUSION

In this letter, the $G/T$ of the TMA was analyzed to explore the noise performance of this structure. It was proposed to switch

the SPDT between the receiver chain and ground so that the noise generated by the RF switch is minimized, which improves the overall $G/T$ of the system. Moreover, the $G/T$ of a practical system with 16 radiating elements was investigated in detail. To explore the performance of the TMA, its $G/T$ was compared with that of a phased array with the same number of antennas. The comparison indicated that the TMA can provide sufficient $G/T$ as a receiver in a wireless communication system.

## REFERENCES

[1] J. D. Fredrick, Y. Wang, and T. Itoh, "Smart antennas based on spatial multiplexing of local elements (smile) for mutual coupling reduction," *IEEE Trans. Antennas Propag.*, vol. 52, no. 1, pp. 106–114, Jan. 2004.

[2] S. Farzaneh and A.-R. Sebak, "Microwave sampling beamformer— prototype verification and switch design," *IEEE Trans. Microw. Theory Techn.*, vol. 57, no. 1, pp. 36–44, Jan. 2009.

[3] M. H. Mazaheri, M. Fakharzadeh, and M. Akbari, "Efficiency enhancement of time-modulated arrays with optimized switching sequences," *IEEE Trans. Antennas Propag.*, vol. 66, no. 7, pp. 3411–3420, Jul. 2018.

[4] X. Xie and Z. Xu, "Direction finding of BPSK signals using time-modulated array," *IEEE Microw. Wireless Compon. Lett.*, vol. 28, no. 7, pp. 618–620, Jul. 2018.

[5] C. He *et al.*, "Direction finding by time-modulated linear array," *IEEE Trans. Antennas Propag.*, vol. 66, no. 7, pp. 3642–3652, Jul. 2018.

[6] G. Li, S. Yang, and Z. Nie, "Direction of arrival estimation in time modulated linear arrays with unidirectional phase center motion," *IEEE Trans. Antennas Propag.*, vol. 58, no. 4, pp. 1105–1111, Apr. 2010.

[7] R. Maneiro-Catoira, J. C. Brégains, J. A. Garcia-Naya, L. Castedo, P. Rocca, and L. Poli, "Performance analysis of time-modulated arrays for the angle diversity reception of digital linear modulated signals," *IEEE J. Sel. Topics Signal Process.*, vol. 11, no. 2, pp. 247–258, Mar. 2017.

[8] Q. Zhu, S. Yang, P. Rocca, and Z. Nie, "Signal-to-noise ratio and time-modulated signal spectrum in four-dimensional antenna arrays," *Microw., Antennas Propag.*, vol. 9, no. 3, pp. 264–270, 2014.

[9] G. Li, S. Yang, Y. Chen, and Z.-P. Nie, "A novel electronic beam steering technique in time modulated antenna array," *Prog. Electromag. Res.*, vol. 97, pp. 391–405, 2009.

[10] P. Rocca, Q. Zhu, E. T. Bekele, S. Yang, and A. Massa, "4-D arrays as enabling technology for cognitive radio systems," *IEEE Trans. Antennas Propag.*, vol. 62, no. 3, pp. 1102–1116, Mar. 2014.

[11] Q. Zhu, S. Yang, R. Yao, and Z. Nie, "Directional modulation based on 4-D antenna arrays," *IEEE Trans. Antennas Propag.*, vol. 62, no. 2, pp. 621–628, Feb. 2014.

[12] C. Sun, S. Yang, Y. Chen, J. Guo, S. Qu, and J. Hu, "4-D retro-directive antenna arrays for secure communication based on improved directional modulation," *IEEE Trans. Antennas Propag.*, vol. 66, no. 11, pp. 5926–5933, Nov. 2018.

[13] M. T. Terrovitis, K. S. Kundert, and R. G. Meyer, "Cyclostationary noise in radio-frequency communication systems," *IEEE Trans. Circuits Syst. I: Fundam. Theory Appl.*, vol. 49, no. 11, pp. 1666–1671, Nov. 2002.

[14] J. Lee, "G/t and noise figure of active array antennas," *IEEE Trans. Antennas Propag.*, vol. 41, no. 2, pp. 241–244, Feb. 1993.

[15] M. H. Mazeri, M. Fakharzadeh, M. Akbari, G. Shaker, and S. S. Naeini, "Interference rejection with time modulated array for GPS application," in *Proc. IEEE Int. Symp. Antennas Propag. USNC/URSI Meeting*, Jul. 2018. pp. 197–198.

[16] Analog Devices, *HMC594LC3B GaAs PHEMT MMIC LOW NOISE AMPLIFIER.* v.03.0514.

[17] Skyworks, *SKY13298-360LF: GaAs SP2T Switch for Ultra Wideband (UWB) 38 GHz.* Rev. C.